Immunological Optimization of a Generic Hydrophobic Pocket for High Affinity Hapten Binding and Diels–Alder Activity

Andrea Piatesi and Donald Hilvert*[a]

Antibody 1E9, which binds a tetrachloronorbornene derivative with subnanomolar affinity and catalyzes the Diels–Alder reaction between tetrachlorothiophene dioxide and N*-ethylmaleimide with high efficiency, arose from a family of highly restricted germ-line immunoglobulins that bind diverse hydrophobic ligands. Two somatic mutations, one at position L89 in the light chain (SerL89Phe) and another at position H47 in the heavy chain (TrpH47Leu), have been postulated to be responsible for the unusually high degree of shape and chemical complementarity observed in the crystal structure of 1E9 complexed with its hapten. To test this hypothesis, the germ-line sequence at these two positions was restored by site-directed mutagenesis. The ensuing 160 to 3900-fold decrease in hapten affinity and the complete loss of catalytic activity support the hypothesis that these somatic mutations substantially remodel the antibody binding pocket. Mutation of the highly conserved hydrogen-bond donor AsnH35, which sits at the bottom of the active site and is a hallmark of this family of antibodies, is also catastrophic with respect to hapten binding and catalysis. In contrast, residues in the CDR H3 loop, which contributes a significant fraction of the hapten-contacting protein surface, have a more subtle influence on the properties of 1E9. Interestingly, while most changes in this loop have neutral or modestly deleterious effects, replacement of MetH100b at the floor of the pocket with phenylalanine leads to a significant sevenfold increase in catalytic activity. The latter result is surprising given the unusually close fit of the parent antibody to the transition-state analogue. Further fine-tuning of the interactions between 1E9 and its ligands by introducing mutations outside the active site could conceivably yield substantially more active catalysts.*

Introduction

Immune recognition is based on shape and chemical complementarity between antibodies and antigens.[1–6] High-affinity interactions are achieved by optimizing receptors from the primary immunoglobulin repertoire by an evolutionary process involving somatic mutation and antigen-driven selection for tight binding.[7,8] The programmable nature of this system makes it a reliable source of tailored receptors for many applications, including catalysis.[9–11]

Antibodies with catalytic properties are obtained when a molecule carrying chemical information about a particular reaction mechanism is used to induce the immune response. For example, the *endo* hexachloronorbornene derivative **1** is an excellent mimic of the transition state for the [4+2] cycloaddition between tetrachlorothiophene dioxide (**2**, TCTD) and *N*-ethylmaleimide (**3**, NEM; Scheme 1). Antibodies that bind this compound catalyze the Diels–Alder reaction efficiently and experience minimal product inhibition

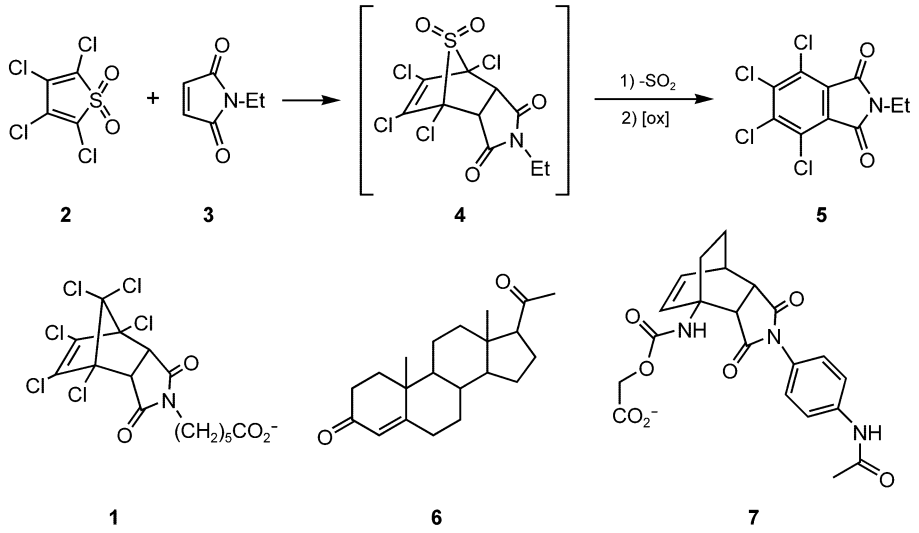

Scheme 1. *Diels–Alder cycloaddition catalyzed by 1E9.[12] The antibody was elicited in response to the tetrachloronorbornene derivative* ***1****. It catalyzes the reaction between tetrachlorothiophene dioxide (****2****) and* N*-ethylmaleimide (****3****) to give the high-energy intermediate* ***4****, which breaks down to yield* N*-ethyltetrachlorophthalimide* ***5****. Progesterone (****6****) and the bicyclo[2.2.2]octene derivative* ***7*** *were used to raise antibodies DB3 and 39-A11, respectively, which are structurally related to 1E9 and derive from the same germ-line genes.*

[a] *A. Piatesi, Prof. Dr. D. Hilvert*
Laboratorium für Organische Chemie
Swiss Federal Institute of Technology (ETH), ETH-Hönggerberg
8093 Zürich (Switzerland)
Fax: (+41) 1-632-1486
E-mail: hilvert@org.chem.ethz.ch

  DOI: 10.1002/cbic.200300806

because of the large structural change that ensues when the initially formed product (**4**) spontaneously eliminates SO_2.[12,13] Structural studies on one such antibody, 1E9, revealed an unusually high degree of structural complementarity between the protein and transition-state analogue (Figure 1 a).[14] Tight packing is achieved through extensive van der Waals contacts and π-stacking interactions (Figure 1 b). In addition, the side chain of AsnH35 at the base of the pocket provides a strategically placed hydrogen bond to the buried succinimide carbonyl group of the hapten. During catalysis, these interactions are believed to preorganize and activate the substrates, on the one hand, and stabilize the transition state enthalpically on the other.[14,15]

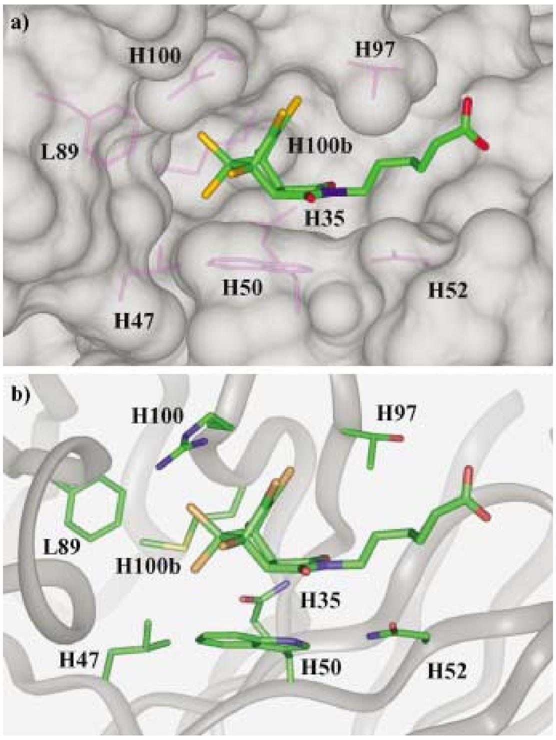

*Figure 1. The 1E9 antibody-combining site with bound hapten **1**. a) Molecular surface representation of the binding pocket showing the excellent shape complementarity between protein and ligand.[14] Under the surface, the side chains of the ligand-contacting residues of the antibody (PheL89, LeuH47, AsnH35, ThrH97, ArgH100, MetH100b) plus AsnH52 at the edge of the active site are shown in pink. b) View of the 1E9 binding site showing all the hapten-contacting residues and their molecular interactions with the hapten.*

The immunological origins of individual antibodies can provide valuable insight into the evolution of binding energy and catalytic function.[16–19] The light and heavy chains of 1E9, for example, derive from the highly restricted V_K5.1 and *VGAM3.8* gene families,[20] which are frequently used to bind small hydrophobic compounds. The encoded germ-line antibodies are believed to possess a polyspecific active site that is optimized for recognition of individual ligands during affinity maturation.[16–19] Mature 1E9 differs from its germ-line precursors by six somatic mutations in the light chain and eight in the heavy chain (Figure 2). Only two of these substitutions, SerL89→Phe and TrpH47→Leu, directly contact the bound hapten (Figure 1 b), and it has been proposed that the ensuing structural changes contribute significantly to the distinctive binding and catalytic properties of 1E9.[14] As is typical for antibodies that bind small molecules, residues of the complementarity-determining region (CDR) H3 of the heavy chain—specifically at positions H97, H100, and H100b—also make extensive contacts with the hapten. Sequence diversity at these sites (Figure 2) may account in part for the divergent properties of 1E9 and other antibodies from the same germ-line families.[14]

To explore the relationship between hapten complementarity and catalytic efficiency in 1E9, we have mutagenized the residues that line the binding pocket, introducing amino acids characteristic of the germ-line sequence or of structurally related antibodies. Our results confirm the importance of somatic mutations at positions L89 and H47 for binding and catalysis by 1E9, as well as the role of the highly conserved AsnH35 as an essential proton donor. They also show that, despite nearly perfect shape complementarity in the starting antibody, significant improvements in catalytic efficacy can still be achieved by mutation within the active site.

Results

The effects of somatic mutations SerL89→Phe and TrpH47→Leu on binding and catalysis

Mature 1E9 is closely related in sequence to antibodies like DB3, which was raised against progesterone (**6**; Scheme 1),[21,22] and 39-A11, which was generated against the bicyclo[2.2.2]oc-

```
VH                              CDR-1                  CDR-2                                                          CDR-3
1E9     QIQLVQSGPELKKPGETVKISCKASGYMFTNYGMNWVKQAPGKALKLMGWINPYTGESTFADDFKGRFAFFLETSATTAYLQINNLKNEDMATYFCARGTTIVRAMDYWGQGTSLTVSS
DB3     ---------------------------A-----V----E----E--W-----I----P-YV---------S-----S----E--------T-----T--DYVNWYF----A--TV----
39-A11  ---------------------------T-----M----Q----G--W-----T----P-YA---------S-----S----Q--------T-----VQAERLRRTF----A--TV----
VFM11   ---------------------------T---------------G--W-----T----P-Y---------S-----S-------------M-----AR

VL                           CDR-1                  CDR-2                                   CDR-3
1E9     DVVMTQTPLSLPVSLGDQASISCRSSQSLVHSNGNTYLHWYLQKPGQSPKFLIYKVSNRFSGVPDRFGGSGSGTDFILKISRVEAEDLGVYFCFQSTHFFPTFGGGTKLEIK
DB3     ------I------N---------------I--------------------L---------Y------S--------T------------I---S--S-VP------------
39-A11  ------T------S---------------L--------------------L---------S------S--------T------------V---S-VT-VP------------
Vκ1A    -----------------------------V--------------------L----------------S--------T----------------S-S--VP
```

Figure 2. Alignment of the amino acid sequences of the heavy (V_H) and light (V_L) chain variable regions of the structurally related antibodies 1E9, DB3, 39-A11 and the germ-line genes VFM11 and $V_κ$1A. Deviations from the 1E9 sequence are highlighted in bold. The heavy-chain germ-line gene of DB3 and 39-A11, VFM9, differs from VFM11 at a single nucleotide; this results in replacement of MetH87 by threonine.[16] This mutation has no effect on hapten binding or catalysis in 1E9.[26] CDR: complementarity-determining region.

tene derivative **7** and catalyzes an unrelated Diels–Alder reaction,[16,23] but it possesses a distinctively shaped active site.[14] Structural comparisons of the three antibodies suggested that the somatic mutations SerL89→Phe and TrpH47→Leu, which are unique to 1E9, dramatically alter the configuration of the binding pocket.[14] Introduction of phenylalanine at position L89 eliminates a prominent cavity present in DB3 and 39-A11, significantly improving shape complementarity between 1E9 and **1**. The substitution of framework residue TrpH47 by leucine is a particularly rare mutation[24] that allows the bulky side chain of TrpH50, which is normally in contact with TrpH47, to rotate about 120° along its C^{α}–C^{β} bond. This conformational change deepens the pocket and creates a flat surface that can π-stack with the succinimide portion of the hapten or with the maleimide substrate. To assess the effects of these changes, the corresponding germ-line residues were introduced into the mature antibody by mutagenesis and the resulting proteins, PheL89Ser and LeuH47Trp, were characterized (Table 1). Incorporating serine at position L89 causes a 160-fold increase in K_d for the hapten and complete loss of catalytic activity. Introducing tryptophan at position H47 leads to a 3900-fold loss in hapten affinity and likewise inactivates the antibody.

Table 1. *Steady-state kinetic parameters and hapten affinity of 1E9 and variants.*[a]

variant	k_{cat} [min^{-1}]	K_{NEM} [mM]	k_{cat}/K_{NEM} [$M^{-1}\,min^{-1}$]	K_d [nM]
1E9 wt[b]	3.7 ± 0.1	9.0 ± 0.6	410	0.10 ± 0.04
PheL89Ser	n.d.[c]	n.d.	n.d.	16 ± 2
LeuH47Trp	n.d.	n.d.	n.d.	390 ± 45
AsnH35Ser	n.d.	n.d.	n.d.	1.3 ± 0.3
AsnH35His	n.d.	n.d.	n.d.	61 000 ± 13 000
AsnH52Lys	2.8 ± 0.1	9.2 ± 1.1	300	0.13 ± 0.06
AsnH52Arg	2.2 ± 0.1	8.4 ± 1.1	260	0.10 ± 0.03
ThrH97Tyr	0.82 ± 0.07	5.7 ± 1.5	140	0.32 ± 0.06
ThrH97Arg	3.9 ± 0.3	15 ± 3	260	0.12 ± 0.02
ArgH100Trp	2.8 ± 0.1	7.0 ± 0.7	400	0.17 ± 0.04
MetH100bPhe[d]	25 ± 1	7.2 ± 1.0	3500	0.08 ± 0.07
MetH100bTrp	1.6 ± 0.1	9.7 ± 1.0	160	0.7 ± 0.10

[a] Kinetic measurements were performed at 25 °C with TCTD (150 μM) in sodium acetate buffer (pH 5.5, 50 mM) containing NaCl (20 mM) and acetonitrile (2%, *v/v*). Fluorescence-quenching titrations were carried out at 15 °C in sodium acetate (pH 5.5, 20 mM) containing NaCl (100 mM). [b] 1E9 wt is a recombinant chimeric Fab, which contains two point mutations (MetH87Thr and GlyL63Ser) for high level production and exhibits kinetic parameters within experimental error of those reported for the original IgG;[26] all mutations were introduced into this background. [c] n.d., not detectable. [d] The kinetic parameters for the MetH100bPhe were confirmed with protein isolated from two independent fermentation runs.

AsnH35 as a strategic hydrogen-bond donor

AsnH35 is one of the hallmark residues of the *VGAM3.8* gene family. It has been postulated to play a key role as a hydrogen-bond donor in ligand recognition and catalysis in 1E9.[14,15] Histidine and serine, which are commonly found at this position in other antibodies,[24] could also conceivably serve as hydrogen-bond donors to the buried carbonyl group of the hapten or the maleimide substrate. However, replacement of AsnH35 with either residue afforded catalytically inactive antibodies possessing substantially decreased affinity (13 to 600 000-fold) for the hapten (Table 1). Both binding and catalysis are evidently highly sensitive to the nature of the hydrogen-bond donor at position H35.

The more exposed carbonyl of the bound hapten in the 1E9 complex does not interact directly with any antibody residue (Figure 1). Conceivably, provision of a hydrogen bond to the corresponding carbonyl of the dienophile might enhance its dienophilicity and further augment catalytic activity.[15] To test this idea, residue AsnH52, which is located on the outside edge of the binding pocket, was replaced by lysine and arginine. Simple modeling studies suggest that these substitutions would position an ammonium or guanidinium group within hydrogen-bonding distance of the solvent-exposed carbonyl without inducing strain into the amino acid side chain or disrupting binding of the hapten to the antibody. Nevertheless, both mutants, AsnH52Lys and AsnH52Arg, are comparable to the parent antibody with respect to hapten affinity and catalysis (Table 1). It is possible that favorable interactions with bound ligand are mitigated by solvation of the exposed side chains.

Hapten-contacting CDR H3 residues

The sequence of 1E9 differs from that of the structurally related antibodies DB3 and 39-A11 most extensively in CDR H3 (Figure 2).[14,16,21] This loop is ten amino acids long in each antibody but exhibits high sequence diversity, reflecting its origin from a different combination of D and J germ-line gene segments and different VDJ junctions. Because the length and overall conformation of this segment is conserved between the antibodies,[14] the side chains oriented away from the binding site play only an indirect role in ligand recognition, whereas those directed into the active site subtly modify the shape of the combining site. The latter point is illustrated by mutagenesis experiments in which the three hapten-contacting CDR H3 residues in 1E9 (ThrH97, ArgH100, and MetH100b) were replaced by the amino acids found at the corresponding positions in DB3 and 39-A11 (Table 1).

The side chain of ThrH97 contacts the portion of the hapten that mimics the dienophile (Figure 1). Its replacement with tyrosine, as in the steroid binder DB3, causes a threefold increase in K_d for the hapten and a fivefold decrease in k_{cat}, whereas an arginine at this position, as in 39-A11, only causes a modest increase in the apparent K_m value for NEM. In contrast, the side chain of ArgH100 interacts directly with the diene component of the hapten (Figure 1). Introducing a tryptophan at this position, as in DB3, leads to a modest increase in K_d for the hapten and small decreases in both k_{cat} and K_{NEM}.

More dramatic results were obtained at position H100b. This residue serves as the floor of the binding pocket and provides a large hydrophobic surface for binding the diene substrate (Figure 1). In 1E9, the flexible aliphatic side chain of methionine occupies this position, whereas in DB3 and 39-A11 the ar-

omatic side chain of phenylalanine is employed. Unexpectedly, substitution of MetH100b with phenylalanine resulted in a substantial sevenfold increase in k_{cat}, from 3.7 min^{-1} to about 25 min^{-1}, with little change in the apparent Michaelis–Menten constant for NEM (Figure 3a, Table 1). Although the K_d values for the hapten obtained in solution by fluorescence quenching are the same within experimental error for this variant and the parent antibody, surface plasmon resonance (SPR) measurements indicate that MetH100bPhe binds the transition-state analogue roughly two times more tightly (Figure 3b). Thus, both antibodies exhibit the same rate constants for ligand association [$k_{on} = (6.1 \pm 1.8) \times 10^4\ s^{-1}\,M^{-1}$ versus $(5.8 \pm 1.6) \times 10^4\ s^{-1}\,M^{-1}$], but the variant has a dissociation rate constant [$k_{off} = (2.6 \pm 0.1) \times 10^{-4}\ s^{-1}$] that is roughly half that of 1E9 itself [$(5.4 \pm 0.1) \times 10^{-4}\ s^{-1}$]. The discrepancy between the SPR and fluorescence titration measurements probably reflects the different nature of interactions between the antibody and a solid support on the one hand and a ligand free in solution on the other.[25,26]

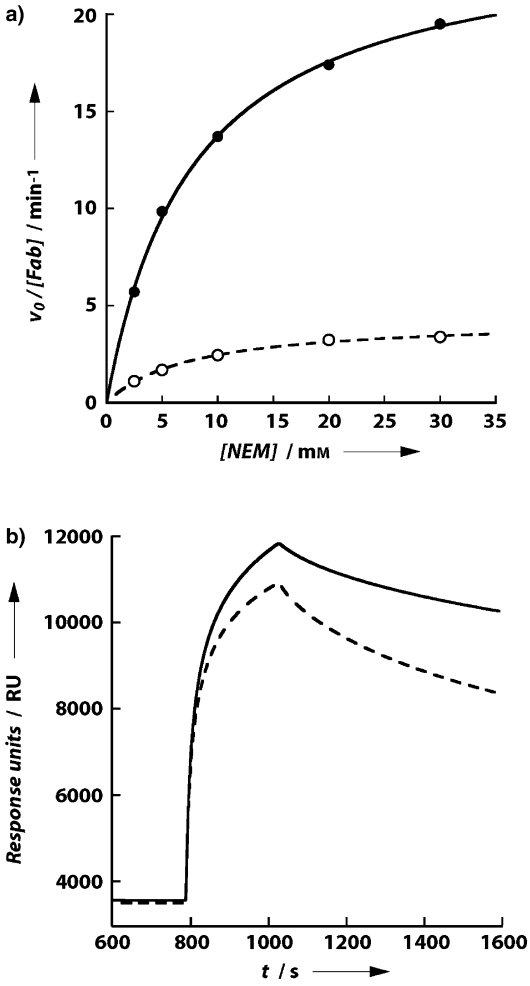

Figure 3. *Comparison of 1E9 and the MetH100bPhe variant. a) Plot of initial rates versus NEM concentration for 1E9 (○) and MetH100bPhe (●). Measurements were carried out in sodium acetate (pH 5.5, 50 mM), sodium chloride (20 mM), and acetonitrile (2% v/v) at 25°C. TCTD concentration was held constant at 150 μM.* b) SPR sensograms for 1E9 (-----) *and MetH100bPhe (——) binding to immobilized transition-state analogue. Measurements were carried out at 25°C at a flow rate of 5 μL min^{-1}. The rate constants* k_{on} *and* k_{off} *were calculated from the association and dissociation phases measured at several Fab concentrations. The sensograms depicted were obtained at [Fab] = 1 μM.*

In contrast to the results obtained with MetH100bPhe, a reduction in ligand affinity and catalytic efficiency is observed when an even bulkier tryptophan residue is introduced at position H100b (Table 1). Although the complexity of the overall reaction sequence makes the interpretation of structure–activity relationships in this system difficult, the activity of the 1E9 variants thus appears to correlate roughly with affinity for the transition-state analogue.

Discussion

Antibody 1E9 shares its basic scaffold with a class of antibodies that recognize small hydrophobic ligands. These include DB3[21,22] and 39-A11,[23] which were raised against progesterone (**6**) and a bicyclo[2.2.2]octene derivative **7**, respectively. It has been suggested[16] that the germ-line precursors of these antibodies encode a generic hydrophobic binding pocket containing a conserved hydrogen-bond donor and that its diversification during affinity maturation affords high-affinity receptors for a large array of structurally diverse molecules. Consistent with this idea, the crystal structures of these antibodies reveal very differently shaped binding pockets,[14] commensurate with their disparate functions.

Comparison of the 1E9, DB3, and 39-A11 crystal structures suggested that a small number of mutations at the combining site, like the SerL89→Phe and TrpH47→Leu substitutions in 1E9, lead to major changes in the shape of the antibody binding pocket.[14] The importance of these two somatic mutations for the recognition of **1** by 1E9 is confirmed by our mutagenesis experiments. Reversion to the germ-line sequence leads to 100 to 1000-fold losses in hapten affinity (Table 1). Residual binding may reflect relatively nonspecific interactions of the ligand with the hydrophobic pocket. Preliminary experiments suggest that these variants, like the germ-line precursor of 39-A11,[16] have an expanded substrate specificity, binding **1** as well as a range of structurally distinct steroid ligands with moderate affinity.[27] Docking studies with mature 1E9 and the anti-progesterone antibody DB3, which also weakly binds **1** but does not catalyze the Diels–Alder reaction between TCTD and NEM, indicate that noncognate ligands bind randomly in the nonpolar pockets, whereas only a single high-affinity binding mode is observed with the parent antibody and its correctly shaped cognate ligand.[14] The loss of hapten affinity is also directly associated with a loss in catalytic function. Both the PheL89Ser and LeuH47Trp variants are catalytically inactive, presumably because the remodeled active sites are unable to preorganize diene and dienophile effectively for bimolecular cycloaddition.

One of the highly conserved amino acids in this family of antibodies is AsnH35, which is positioned to donate a hydrogen bond to the carbonyl group of the ligand in each of the antibody–hapten complexes. This residue provides a key polar interaction in an otherwise hydrophobic environment and helps bind the cognate ligand in a specific orientation. As found pre-

viously with 39-A11,[28] AsnH35 is absolutely essential for the catalytic activity of 1E9 (Table 1), presumably because it helps to orient the maleimide for reaction and enhance its dienophilicity.[15] Even relatively conservative substitutions with serine or histidine lead to major losses of activity. Unfortunately, as seen previously with 39-A11,[28] attempts to further activate the dienophile by engineering additional hydrogen bonding interactions with its solvent-exposed carbonyl group have not been successful (Table 1).

While the residues at position H35, H47, and L89 have a profound influence on the properties of 1E9, the hapten-contacting CDR H3 residues, which constitute a large fraction of the hydrophobic active-site binding surface (Figure 1), modulate antibody complementarity more subtly. The small decreases in hapten affinity and/or catalytic activity upon substitution of the hapten-contacting residues H97 and H100 are hardly surprising, but the sevenfold increase in k_{cat} observed for the MetH100bPhe mutant was unexpected in light of the snug fit between hapten and protein in the starting structure. The rigid aromatic side chain of phenylalanine may pack the substrates better than the more flexible aliphatic side chain of methionine or the bulkier side chain of tryptophan, reducing their rotational and translational degrees of freedom. However, the effect is very subtle, since hapten affinity is increased at most twofold by this mutation.

Overall, our results suggest that a small number of somatic mutations, coupled with minor adjustments in CDR H3 residues, are sufficient to convert a relatively nonspecific antibody-binding site into a highly selective receptor and catalyst. Given the already excellent fit of **1** to the mature 1E9 antibody, future improvements with respect to hapten binding and catalytic activity will probably require mutations distant from the active site. In vitro selection experiments with antibody libraries displayed in various formats,[29–33] which have successfully converted nanomolar binders to receptors with picomolar to femtomolar affinities, will be particularly useful in this regard. Insofar as **1** is a good mimic of the presumed Diels–Alder transition state,[14] a significant fraction of the binding energy gained may well be manifest as higher catalytic efficiency.

Experimental Section

Tetrachlorothiophene dioxide (TCTD)[34] and hapten **1**[12] were synthesized according to published protocols and gave satisfactory spectroscopic data. *N*-Ethylmaleimide (NEM) was obtained from Aldrich. *E. coli* XL1-blue and TOPP2 strains were obtained from Stratagene (La Jolla, CA). Restriction endonucleases and T4 DNA ligase were purchased from New England Biolabs (Beverly, MA) and Fermentas (Vilnius, Lithuania), respectively. Polymerase chain reactions (PCRs) were carried out with thermostable HotStarTaq DNA polymerase from Qiagen (Basel, Switzerland). Oligonucleotides for mutagenesis and sequencing were prepared by Microsynth (Balgach, Switzerland). All nucleic acid manipulations were according to standard procedures.[35] DNA sequencing was performed on an ABI PRISM 310 Genetic Analyzer from PE-Applied Biosystems (Foster City, CA).

Site-Directed Mutagenesis: Plasmid p4xH-1E9(MetH87Thr/GlyL63Ser), which was previously constructed for optimized production of the chimeric 1E9 Fab fragment in *E. coli*,[26] served as a template for site-directed mutagenesis. Substitutions were generally chosen to exploit the most frequently used codon for a particular amino acid among highly expressed genes in *E. coli* (Wisconsin Sequence Analysis package, version 8, Genetics Computer Group, Inc.). Except for the ArgH100Trp and MetH100bPhe mutants, site-directed mutagenesis was accomplished by a standard overlap-extension PCR technique with the following primers: 1E9 V_L flanking sense (5′-GCGTACGCTGAGCTCGTGATGACCCAGACTCCACTCTCC-3′, *Sac*I site underlined) and antisense (5′-TTTGATCTCAAGCTTGGTGCCACCACCGAACGTCGGAAA-3′, *Hind*III site underlined); 1E9 V_H flanking sense (5′-GTGTTAAGCTGGGGATCCTCTAGAGGTTGA-3′, *Bam*HI site underlined) and antisense (5′-GGCTGAGGAGACGGTGACCGAGGTTCCTTG-3′, *Bst*EII site underlined); PheL89Ser mutagenic sense (5′-GATTTGGGAGTTTATTTCTGT**TCC**CAAAGTACA-3′) and antisense (5′-TGTACTTTG**GGA**ACAGAAATA-3′); AsnH35His mutagenic sense (5′-TATGGAATG**CAC**TGGGTGAAG-3′) and antisense (5′-CTTCACCCA**GTG**CATTCCATA-3′); AsnH35Ser mutagenic sense (5′-TATGGAATG**TCC**TGGGTGAAG-3′) and antisense (5′-CTTCACCCA**GGA**CATTCCATA-3′); LeuH47Trp mutagenic sense (5′-GCTTTAAAG**TGG**ATGGGCTGG-3′) and antisense (5′-CCAGCCCAT**CCA**CTTTAAAGC-3′); AsnH52Arg mutagenic sense (5′-ATGGGCTGGATA**CGT**CCCTACACTGGA-3′) and antisense (5′-TCCAGTGTAGGG**ACG**TATCCAGCCCAT-3′); AsnH52 Lys mutagenic sense (5′-ATGGGCTGGATA**AAA**CCCTACACTGGA-3′) and antisense (5′-TCCAGTGTAGGG**TTT**TATCCAGCCCAT-3′); ThrH97Arg mutagenic sense (5′-TATTTCTGTGCAAGGGGGACT**CGT**ATAGTGA-3′) and antisense (5′-CCTCACTAT**ACG**AGTCCCCCTT-3′); ThrH97Tyr mutagenic sense (5′-TATTTCTGTGCAAGGGGGACT**TAC**ATAGTGA-3′) and antisense (5′-CCTCACTAT**GTA**AGTCCCCCTT-3′). The mutagenized positions in the primers are denoted in bold. Because of the proximity of the site of mutation and the 3′ *Bst*EII restriction site, the ArgH100Trp and MetH100bPhe mutations were introduced in one PCR step by using mutagenic antisense primers containing the restriction site in combination with the 1E9 V_H flanking sense primer. The antisense primers were 5′-GACGGTGACCGAGGTTCCTTGACCCCAGTAGTCCATAGC**CCA**CACTAT-3′ for ArgH100Trp and 5′-GACGGTGACCGAGGTTCCTTGACCCCAGTAGTC**GAA**AGCCCT-3′ for MetH100bPhe (*Bst*EII sites are underlined and mutagenized positions denoted in bold). Constructs were confirmed by DNA sequencing with the HSEQF, HSEQB, and LSEQB primers, as previously described.[26]

Production, Purification, and Characterization of Chimeric Fab Fragments: Large-scale antibody production was achieved by transforming the TOPP2 *E. coli* strain with p4xH-1E9 (MetH87Thr/GlyL63Ser) and its mutagenized derivatives, followed by high-density fermentation (2 L) in a BIOFLO 3000 Bioreactor (New Brunswick Scientific, Edison, NJ) as previously described.[26,36] The chimeric Fab fragments were purified from crude periplasmic lysates by protein G affinity chromatography, followed by Mono S cation-exchange chromatography. Sample purity was assessed by SDS PAGE. Protein concentration was determined spectroscopically at 280 nm, by using molar absorption coefficients calculated as described by Pace.[37] An ε_{280} of 59 000 $M^{-1}cm^{-1}$ was assumed for all but the LeuH47Trp, ThrH97Tyr, and ArgH100Trp mutants, which had calculated extinction coefficients of 64 500, 60 500, and 64 500 $M^{-1}cm^{-1}$, respectively. With the exception of the MetH100bPhe mutant, which was stored at −80 °C, all the Fab variants were stored at 4 °C in 20 mM Tris-HCl (pH 7.2) containing EDTA 0.5 mM and NaCl 100 mM. The final yield of the chimeric Fab 1E9(MetH87Thr/GlyL63Ser) was approximately 4 mg L^{-1}, while that of the mutants varied between 1.5 and 7 mg L^{-1}.

Kinetic assays: The reaction between TCTD and NEM was carried out at 25 °C in sodium acetate buffer (pH 5.5, 50 mM) containing NaCl (20 mM) in the presence (typically 0.1 to 1.0 μM) or absence

of antibody. The substrates were diluted from stock solutions in acetonitrile; the final concentration of acetonitrile in the reaction mixture was 2% by volume. Initial velocities were determined by starch–I_2 bleaching at 606 nm at several concentrations of NEM while holding the concentration of TCTD constant at 150 μM.[26,38] The data were corrected for the uncatalyzed reaction and fitted to the Michaelis–Menten Equation:

$$v_o/[Ab] = \frac{k_{cat}[NEM]}{K_{NEM} + [NEM]} \quad (1)$$

here v_o is the initial rate, [Ab] and [NEM] are the active site and substrate concentrations, and k_{cat} and K_{NEM} are the apparent catalytic rate and Michaelis constants at a fixed concentration of diene.

Hapten-binding assays: Hapten dissociation constants (K_d) for the Fab mutants were determined as previously described.[26,39] Titration curves were recorded by stepwise addition of a ligand stock solution to a diluted solution of the chimeric Fab fragment (26 nM) and subsequent measurement of the fluorescence. With the exception of the LeuH47Trp, PheL89Ser, and AsnH35His mutants, a hapten stock solution of 15 μM in buffer was used for all the Fab variants. The LeuH47Trp and PheL89Ser mutants were characterized by using a 150 μM hapten stock solution in buffer, whereas a 15 mM hapten stock solution in neat acetonitrile was used for AsnH35His. The excitation and emission wavelengths were 290 nm and 340 nm, respectively, and the corresponding band passes were 8 nm and 16 nm. The high voltage of the detector was set to 900 V. These measurements were carried out in sodium acetate (pH 5.5, 20 mM) and NaCl (100 mM) at 15 °C. The dissociation constant (K_d) for the Fab–ligand complex was calculated by nonlinear least-squares fitting of the observed fluorescence (F) obtained at various ligand concentrations (L_T) to Equation (2)

$$F = F_E - [(E_T + L_T + K_d) - [(E_T + L_T + K_d)^2 - 4E_TL_T]^{1/2}] \times (F_E - F_{EL})/2E_T \quad (2)$$

here E_T is the total Fab concentration, F_E is the observed fluorescence intensity without any ligand, and F_{EL} is the fluorescence intensity of the Fab-ligand complex at infinite ligand concentration.

Surface plasmon-resonance measurements: The binding of hapten to chimeric 1E9 Fab and the MetH100bPhe mutant was monitored by the surface plasmon-resonance (SPR) technique with a BIAcore 3000 instrument (Pharmacia, Uppsala, Sweden).[40,41] All experiments were performed at 25 °C. The surface of the dextran chip was activated with 1-[3-dimethylaminopropyl]-3-ethylcarbodiimide hydrochloride and *N*-hydroxysuccinimide in acetate (pH 4.0, 10 mM) and covalently linked to the borine serum albumin (BSA)–hapten conjugate (SPR response: 4000 RU). Fab samples were diluted in HEPES buffer (pH 7.4, 10 mM) containing NaCl (150 mM), EDTA (3 mM), and polysorbate 20 (0.005%, *v/v*) prior to SPR analysis. The Fab fragments were injected in the presence of the immobilized hapten at a flow rate of 5 μL min^{-1}. The association rate constant (k_{on}) was determined by measuring the rate of binding to the hapten at three different Fab concentrations (1 μM, 0.6 μM, 0.4 μM). The dissociation phase (k_{off}) was monitored after the association process was complete. The dextran matrix was regenerated after each injection by using aq. HCl (100 mM). Rate constants were calculated from the SPR data by using BIAevaluation 3.1 software (Pharmacia, Uppsala, Sweden). A single-site binding model (A + B = AB) was assumed for the analysis.

Acknowledgements

This work was supported by the ETH Zürich and Novartis Pharma AG. We are grateful to J. Scheuermann and D. Neri for assistance with BIAcore measurements, J. Goldberg and A. Herrmann for valuable discussions, and A. Aemissegger for help preparing the graphics.

Keywords: affinity maturation · antibody catalysis · Diels–Alder reaction · germ-line antibody · surface plasmon resonance (SPR)

[1] E. A. Kabat, *Structural Concepts in Immunology and Immunochemistry*, Holt, Rinehart, and Winston, New York, NY, **1976**.
[2] D. Pressman, A. Grossberg, *The Structural Basis of Antibody Specificity*, Benjamin, New York, NY, **1968**.
[3] A. Nisonoff, J. Hopper, S. Spring, *The Antibody Molecule*, Academic Press, New York, NY, **1975**.
[4] E. J. Sundberg, R. A. Mariuzza, *Adv. Protein Chem.* **2003**, *61*, 119.
[5] I. A. Wilson, R. L. Stanfield, *Curr. Opin. Struct. Biol.* **1993**, *3*, 113.
[6] D. R. Davies, G. H. Cohen, *Proc. Natl. Acad. Sci. USA* **1996**, *93*, 7.
[7] F. W. Alt, T. K. Blackwell, G. D. Yancopoulos, *Science* **1987**, *238*, 1079.
[8] K. Rajewsky, I. Förester, A. Cumang, *Science* **1987**, *238*, 1088.
[9] D. Hilvert, *Annu. Rev. Biochem.* **2000**, *69*, 751.
[10] P. G. Schultz, R. A. Lerner, *Science* **1995**, *269*, 1835.
[11] P. G. Schultz, J. Yin, R. A. Lerner, *Angew. Chem.* **2002**, *114*, 4607; *Angew. Chem. Int. Ed.* **2002**, *41*, 4427.
[12] D. Hilvert, K. W. Hill, K. D. Nared, M.-T. M. Auditor, *J. Am. Chem. Soc.* **1989**, *111*, 9261.
[13] G. MacBeath, D. Hilvert, *J. Am. Chem. Soc.* **1994**, *116*, 6101.
[14] J. A. Xu, Q. L. Deng, J. G. Chen, K. N. Houk, J. Bartek, D. Hilvert, I. A. Wilson, *Science* **1999**, *286*, 2345.
[15] J. G. Chen, Q. L. Deng, R. X. Wang, K. N. Houk, D. Hilvert, *ChemBioChem* **2000**, *1*, 255.
[16] F. E. Romesberg, B. Spiller, P. G. Schultz, R. C. Stevens, *Science* **1998**, *279*, 1929.
[17] H. D. Ulrich, E. Mundorff, B. D. Santarsiero, E. M. Driggers, R. C. Stevens, P. G. Schultz, *Nature* **1997**, *389*, 271.
[18] G. J. Wedemayer, P. A. Patten, L. H. Wang, P. G. Schultz, R. C. Stevens, *Science* **1997**, *276*, 1665.
[19] P. A. Patten, N. S. Gray, P. L. Yang, C. B. Marks, G. J. Wedemayer, J. J. Boniface, R. C. Stevens, P. G. Schultz, *Science* **1996**, *271*, 1086.
[20] M. R. Haynes, M. Lenz, M. J. Taussig, I. A. Wilson, D. Hilvert, *Isr. J. Chem.* **1996**, *36*, 151.
[21] J. H. Arevalo, E. A. Stura, M. J. Taussig, I. A. Wilson, *J. Mol. Biol.* **1993**, *231*, 103.
[22] J. H. Arevalo, M. J. Taussig, I. A. Wilson, *Nature* **1993**, *365*, 859.
[23] A. C. Braisted, P. G. Schultz, *J. Am. Chem. Soc.* **1990**, *112*, 7430.
[24] E. A. Kabat, T. T. Wu, H. M. Perry, K. S. Gottesman, C. Foeller, *Sequences of Proteins of Immunological Interest*, 5th ed., U.S. Public Health Service, National Institutes of Health, Bethesda, MD, **1991**.
[25] A. Huber, S. Demartis, D. Neri, *J. Mol. Recognit.* **1999**, *12*, 198.
[26] A. Piatesi, D. Hilvert, *Can. J. Chem.* **2002**, *80*, 657.
[27] A. Piatesi, C. Aldag, unpublished results.
[28] F. E. Romesberg, P. G. Schultz, *Bioorg. Med. Chem. Lett.* **1999**, *9*, 1741.
[29] E. T. Boder, K. S. Midelfort, K. D. Wittrup, *Proc. Natl. Acad. Sci. USA* **2000**, *97*, 10701.
[30] J. Hanes, L. Jermutus, S. Weber-Bornhauser, H. R. Bosshard, A. Plückthun, *Proc. Natl. Acad. Sci. USA* **1998**, *95*, 14130.
[31] R. E. Hawkins, S. J. Russell, G. Winter, *J. Mol. Biol.* **1992**, *226*, 889.
[32] W. P. Yang, K. Green, S. Pinzsweeney, A. T. Briones, D. R. Burton, C. F. Barbas III, *J. Mol. Biol.* **1995**, *254*, 392.
[33] R. Schier, A. McCall, G. P. Adams, K. W. Marshall, H. Merritt, M. Yim, R. S. Crawford, L. M. Weiner, C. Marks, J. D. Marks, *J. Mol. Biol.* **1996**, *263*, 551.
[34] M. S. Raasch, *J. Org. Chem.* **1980**, *45*, 856.

[35] J. Sambrook, E. F. Fritsch, T. Maniatis, *Molecular Cloning. A Laboratory Manual*, Cold Spring Harbor Laboratory Press, Cold Spring Harbor, New York, **1989**.
[36] H. D. Ulrich, P. A. Patten, P. L. Yang, F. E. Romesberg, P. G. Schultz, *Proc. Natl. Acad. Sci. USA* **1995**, *92*, 11907.
[37] C. N. Pace, F. Vajdos, L. Fee, G. Grimsley, T. Gray, *Protein Sci.* **1995**, *4*, 2411.
[38] Y. Gozin, D. Hilvert, *Helv. Chim. Acta* **2002**, *85*, 4328.
[39] K. Taira, S. J. Benkovic, *J. Med. Chem.* **1988**, *31*, 129.
[40] H. Kobayashi, H. Morioka, K. Tobisawa, T. Torizawa, K. Kato, I. Shimada, O. Nikaido, J. D. Stewart, E. Ohtsuka, *Biochemistry* **1999**, *38*, 532.
[41] U. Jönsson, L. Fägerstam, B. Ivarsson, B. Johnsson, R. Karlsson, K. Lundh, S. Löfäs, B. Persson, H. Roos, I. Rönnberg, S. Sjölander, E. Stenberg, R. Stählberg, C. Urbaniczky, H. Östlin, M. Malmqvist, *Biotechniques* **1991**, *11*, 620.

Received: October 27, 2003 [F 806]

